OPEN ACCESS Freely available online

PLOS ONE

Detection of Osteogenic Differentiation by Differential Mineralized Matrix Production in Mesenchymal Stromal Cells by Raman Spectroscopy

Pei-San Hung[1☯], Yi-Chun Kuo[2☯], He-Guei Chen[1], Hui-Hua Kenny Chiang[1,3], Oscar Kuang-Sheng Lee[4,5]*

1 Institute of Biophotonics, National Yang-Ming University, Taipei, Taiwan, **2** Institute of Clinical Medicine, National Yang-Ming University, Taipei, Taiwan, **3** Institute of Biomedical Engineering, National Yang-Ming University, Taipei, Taiwan, **4** Department of Orthopaedics and Traumatology, Taipei Veterans General Hospital, Taipei, Taiwan, **5** Stem cell Research Center, National Yang-Ming University, Taipei, Taiwan

Abstract

Mesenchymal stromal cells (MSCs) hold great potential in skeletal tissue engineering and regenerative medicine. However, conventional methods that are used in molecular biology to evaluate osteogenic differentiation of MSCs require a relatively large amount of cells. Cell lysis and cell fixation are also required and all these steps are time-consuming. Therefore, it is imperative to develop a facile technique which can provide real-time information with high sensitivity and selectivity to detect the osteogenic maturation of MSCs. In this study, we use Raman spectroscopy as a biosensor to monitor the production of mineralized matrices during osteogenic induction of MSCs. In summary, Raman spectroscopy is an excellent biosensor to detect the extent of maturation level during MSCs-osteoblast differentiation with a non-disruptive, real-time and label free manner. We expect that this study will promote further investigation of stem cell research and clinical applications.

Citation: Hung P-S, Kuo Y-C, Chen H-G, Chiang H-HK, Lee OK-S (2013) Detection of Osteogenic Differentiation by Differential Mineralized Matrix Production in Mesenchymal Stromal Cells by Raman Spectroscopy. PLoS ONE 8(5): e65438. doi:10.1371/journal.pone.0065438

Editor: Shree Ram Singh, National Cancer Institute, United States of America

Received January 7, 2013; **Accepted** April 24, 2013; **Published** May 29, 2013

Funding: This work was supported in part by the UST-UCSD International Center of Excellence in Advanced Bio-engineering sponsored by the Taiwan National Science Council I-RiCE Program under Grant Number: NSC100-2911-I-009-101. The authors also acknowledge financial support from the Taipei Veterans General Hospital (VGH101E1-012, VGH101C-015 and VN101-07), the National Science Council, Taiwan (NSC100-2120-M-010-001, NSC100-2314-B-010-030-MY3, NSC100-2321-B-010-019, NSC 101-2911-I-010-503, and NSC 99-3114-B-002-005), the Ministry of Economic Affairs, Taiwan (101-EC-17-A-17-S1-203), and a Grant from National Research Program for Biopharmaceuticals (DOH101-TD-PB-111-NSC014), as well as the National Yang-Ming University/Cheng Hsin General Hospital Grant (101F195CY07). This study was also supported by the Aim for the Top University Plan from the Ministry of Education. The funders had no role in study design, data collection and analysis, decision to publish, or preparation of the manuscript.

Competing Interests: The authors have declared that no competing interests exist.

* E-mail: kslee@vghtpe.gov.tw

☯ These authors contributed equally to this work.

Introduction

Mesenchymal stromal cells (MSCs) are multipotent adult stem cells which were first discovered by Friedenstein's group in bone marrow stoma as fibroblast-like non-hematopoietic stem cells [1] and have the capacity to differentiate into osteocytes, adipocytes, endothelial cells, myocytes, astrocytes, and hepatocytes.[2,3,4,5,6] MSCs have been isolated from a variety of tissue such bone marrow, umbilical cord blood, [7] adipose tissue, [8] and peripheral blood.[9,10] Previous studies have shown that MSCs play an important role during bone formation and bone remodeling and also have been indicated as potential resources for many clinical applications. [11,12,13,14]

An osteoblast is bone forming cell which mediates in the bone-homeostasis during osteogenesis [15] and exhibits a typical elongated fibroblast-like morphology with a spindle-like appearance. It has been reported that various extracellular matrices and soluble factors modulated the activity of signaling proteins [16] and transcription factors [17] during MSCs-osteoblast differentiation. Current strategies to induce MSCs osteogenesis include mechanical factors such as matrix stiffness [18,19] and chemical stimuli such as β-glycerol phosphate, [7] dexamethasone,[20] and ascorbic acid. [21] The mineral matrices which produce by bone cells are widely applied in tissue engineering and regenerative medicine researches for enhancement of osteogenesis or as maturation biomarkers of MSC-osteoblast differentiation. [22,23,24,25,26]

To evaluate the maturation level of MSCs-osteoblast differentiation of, histochemical and molecular biological methods such as alkaline phosphatase staining, Von Kossa staining, Western blot and reverse transcription polymerase chain reaction (RT-PCR) are commonly used.[27,28,29] However, all these traditional methods are time-consuming, cell-destructing, and can only offer semi-quantitative or non-quantitative information except for real-time RT-PCR. Moreover, these conventional methods to detect the extent of osteogenic differentiation are not in situ and require cell lyses or fixation, which causes cell death and makes continuous observation very difficult. A sensitive and objective method for research studies and clinical applications is not still available.

Progress has been achieved to introduce vibrational spectroscopy including Raman and Infrared spectroscopy (IR) into medical diagnostics and cellular biology over the past decade. Most of the clinical diagnostics carry out with infrared microspectroscopy which offers much higher speed and a spatial resolution

of about the size of a cell.[30,31] However, water or liquid solvents cannot be used during IR measurement and sample preparation should be elaborate. To investigate the chemical and biological properties changes during bone formation process in MSCs, Raman spectroscopy has been used in this study due to its high spatial resolution, high sensitive of biological changes at a subcellular level detection and the sample for Raman measurement can be almost in any state. [32,33]

Raman spectroscopy has been widely used as an in situ and single cell detector for a wide variety of biological applications recently. [34,35,36]The Raman spectroscopic technique provides a detail molecular structure, chemical composition and molecular interaction in tissues and cells.[37,38,39,40,41] The molecular composition and structural changes, concomitant with the disease progression, are often revealed in the spectra. Hence, any set of quantitative spectral changes, sufficiently specific to a particular state of differentiation, can be used as phenotypic markers of the disease.[42] Previous studies have illustrated the differences between Raman spectra of the healthy vs. the diseased cells or tissues, [43,44] and the feasibility of Raman spectroscopic fingerprinting of cells for clinical diagnostic applications has been successfully demonstrated.[43,44,45,46]

The potential of Raman spectroscopic technique is evaluated to detect the maturation level during MSCs-osteoblast differentiation in live cells through detecting the extent of mineralized matrices which are reported to possibly be involved in osteogenesis including amorphous calcium phosphate (ACP)[47], octacalcium phosphate (OCP)[48], hydroxyapatite (HAP)[49,50], β-tricalcium phosphate (β-TCP) [51] and dicalcium phosphate dehydrate (DCPD) [51] in this study.

Materials and Methods

Culture maintenance and expansion

For studies involving human tissues we obtained Institutional Review Board approval of Taipei Veterans General Hospital with written informed consents. MSCs were isolated from bone marrow collected from healthy young donors during fracture surgery, and purified with negative immuno-selection and limiting dilution as previously described.[7] Expansion medium for MSCs consists of Iscove's Modified Dulbecco's medium (IMDM; Gibco, Grand Island, NY) and 10% ES fetal bovine serum (ES-FBS; Sigma-Aldrich, St Louis, MO), supplemented with 10 ng/ml basic fibroblast growth factor (bFGF; R&D systems, Inc., Minneapolis, MN), 10 ng/ml epidermal growth factor (EGF; R&D system, Inc.), 100 U penicillin, 1000 U streptomycin, and 2 mM L-glutamine (PSG; Gibco).

Osteogenic differentiation of MSCs

Osteogenic induction was carried out according to previously reported protocols [29]. To induce osteogenic differentiation, MSCs were cultured to the density of approximately 40% confluence before treatment with the osteogenic induction medium consisting of IMDM supplemented with 0.1 μM dexamethasone (Sigma-Aldrich), 10 mM β-glycerol phosphate (Sigma-Aldrich), and 0.2 mM ascorbic acid (ASA; Sigma-Aldrich). MSCs were treated with osteogenic medium for 24 days in which medium was changed every 3 days.

RNA extraction and real-time polymerase chain reaction (qPCR)

RNA prepared from $3x10^5$ in vitro culture cells and total RNA was isolated using Trizol (Invitrogen) and cleaned using an RNA easy minikit (Quiagen, Courtaboeuf, France). We reverse transcribed the messenger RNA to complementary DNA using reagents (Genemark Technology, Taiwan) according to the manufacturer's instructions. Quantitative real-time PCR analysis of total RNA from cultured cells was performed using ABI Step One Plus Real Time PCR System. cDNA was amplified using an ABI Step One Plus Real Time PCR System at 95°C for 60 seconds, 56°C for 45 seconds, and 72°C for 60 seconds for 40 cycles, after initial denaturation at 95°C for 5 minutes. The primers used for amplification are 5′-gtgcctaggcgcatttca-3′ (forward) and 5′-gctcttcttactgagagtggaagg-3′ (reverse) for runt-related transcription factor 2 (RUNX2); 5′-gaaccaaaaattaaagtgattgaagg-3′ (forward) and 5′-tgacttttgttagtgtgggtcct-3′ (reverse) for periostin, 5′-cccctggaaagaatggagat-3′ (forward) and 5′-aatcctcgagcaccctgag-3′ (reverse) for type I collagen; internal control, 5′-gctggcccatagtgatcttt-3′ (forward) and 5′-tccttgggttatcttcacacg-3′ (reverse) for TATA-binding protein (TBP). The relative expression levels of mRNA in cells were normalized by internal controls, non-differentiated controls and determined with ΔΔCT.

Cytochemical staining of osteogenic differentiation

For histochemical analysis of osteogenesis, cells were rinsed twice with phosphate buffered saline (PBS), fixed with 3.7% formaldehyde for 20 minutes, and washed with distilled water. Mineralization matrix was analyzed with Von kossa staining using 1% silver nitrate (Sigma-Aldrich) under UV light for 45 minutes, followed by 3% sodium thiosulfate (Sigma-Aldrich) for 5 minutes, and then counterstained with van Gieson (Sigma-Aldrich) for 5 minutes and with Alkaline phosphatase histochemical stain using the BCIP/NBT (5-bromo-4-chloro-3-indolyl phosphate/nitroblue tetrazolium; Sigma-Aldrich) solution in dark for 45 minutes.

Raman spectroscopy

In this study, a 18-mW He-Ne laser operating at 632.8 nm was used to provide the Raman excitation. An 80-cm focal length spectrometer system (LabRAM HR 800, Jobin Yvon, Longjumeau Cedex, France) was equipped with a BX-41 Olympus confocal optical microscope and a 60X water immersion M-Plan objective (NA = 0.9). A liquid-nitrogen-cooled CCD 2D array detector was used to measure the Raman signal by integrating for 30 second. Spectra were recorded from 800 to 1800 cm^{-1} with a spectral resolution of approximately 5 cm^{-1}.

Specimen preparation

MSCs seeded on 2 mm×2 mm quartz coverslip and treated osteogenic induction medium. Before measurement, cells were washed with PBS for twice, and the coverslip was placed on quartz slide. An O-ring placed between coverslip and slide. The minimized chamber was filled with PBS to prevent cell death during the measurement, as was shown in Figure 1.

Data analysis

Each Raman spectrum represents the average of 5 different replicates on one single cell surface. Labspec 5.0 software was used for signal processing. All spectra in this study were normalized to CH_2 wag at 1449 cm^{-1}. A Phe background spectrum at 1004 cm^{-1} was acquired for each individual substrate used, and subsequently subtracted before averaging. [41,52,53,54,55,56,57,58]

Results

Raman signals of background

The background signals of quartz slide and quartz slide with coverslip have been found at 800 cm^{-1} and 1065 cm^{-1} (Figure S1). To subtract the compounds from the background, we took the

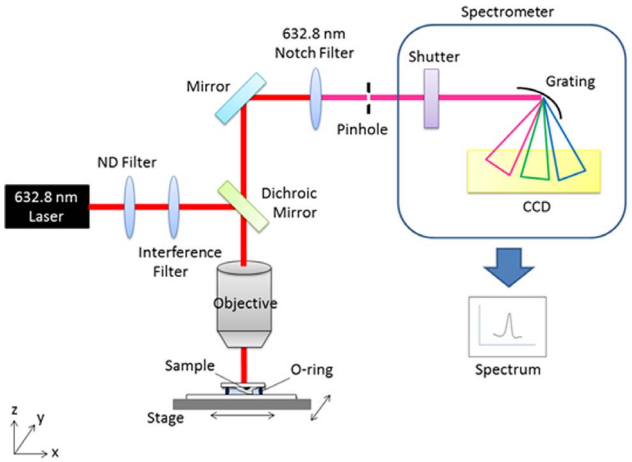

Figure 1. Schematic diagram of the Raman platform set-up.
doi:10.1371/journal.pone.0065438.g001

Raman spectrum of background signal from quartz slide, quartz slide combined with quartz coverslip in air, and MSC growth medium and MSC with growth medium which were obtained by averaging over 5 different locations for 30 seconds integration time. The Raman signal of cellular component, Phenylalanine (Phe), at 1004 cm^{-1} is significantly higher in MSCs compared to control groups. Our results show that mineralized matrix signals in cells are not interfered with background signals, as was shown in Figure 2. These findings indicated that experimental setup of Raman spectroscopy is a great tool for detecting the mineralized matrix signals specifically in live cells during MSC-osteoblast differentiation.

Raman spectra of MSCs and MSCs-derived osteoblasts

In order to elucidate the differential production of mineralized matrix during osteogenic differentiation of MSCs, Raman spectra were recorded on day 0, 3, 9, 15 and day 24 for three times, and a consist result which was shown in Figure 3A. The region of Raman spectra of cellular components and mineral species were marked in yellow. Previous studies have demonstrated that OCP is the precursor of mineralized matrix at the early stage mineralization and also involve in HAP synthesis during bone formation.[59,60] The Raman signal of OCP at 957cm^{-1} shows in MSCs at Day 0 without osteogenic induction and signal intensity decreases from Day 3 after osteogenic induction. The OCP signal cannot be detected after Day 9 osteogenic induction. In addition, a Raman signal of β-TCP at 970 cm^{-1}, is a HAP precursor, is found after Day 9 osteogenic induction (Figure 3B).[61] As expected, the intensity of Raman signal of HAP at 960 cm^{-1} slightly increase after Day 9 and highly correlates with induction time from day 9 to Day 24. According to our data, OCP might be dissolved for mineralization. As the result of that OCP signal can be used as precursor marker which shows in non-differentiated MSCs and slightly decreases when cells underwent oesteogenic differentiation. Furthermore, β-TCP contributes to HAP synthesis which can be used as an early stage marker for MSC-osteoblast differentiation so the intensity of β-TCP signal rises at Day 9 under osteogenic induction and quickly disappeared afterward.

The signals of ACP and DCPD are undetectable throughout the experiments. The Raman spectrum in Figure 3A consisting of peaks corresponding to the molecular vibration of various cellular components including of Phe at 1004 cm^{-1}, amide I at 1660 cm^{-1}, and carbohydrate CH_2 wag at 1449 cm^{-1} were observed. Under osteogenic induction, the HAP signal increases significantly at 960 cm^{-1}. To investigate the expression levels of mineral components in MSCs during osteogenic differentiation, we magnified Fig. 3A. As show in Fig. 3B, Raman spectrum was dissected in detail as depicted in the region from 900 to 1020 cm^{-1}. These data shows that OCP at 957 cm^{-1} represent is significantly higher in the undifferentiated MSCs, but decreased quickly after 6th day of osteogenic induction which data was not shown. The OCP signal cannot be found after day 9. On the contrary, we found the β-TCP at 970 cm^{-1} transient appears at the Day 9. The Raman signal of HAP at 960 cm^{-1} dramatically increased from Day 9 under osteogenic induction in MSCs. These results demonstrate that Raman spectroscopy is a powerful tool to

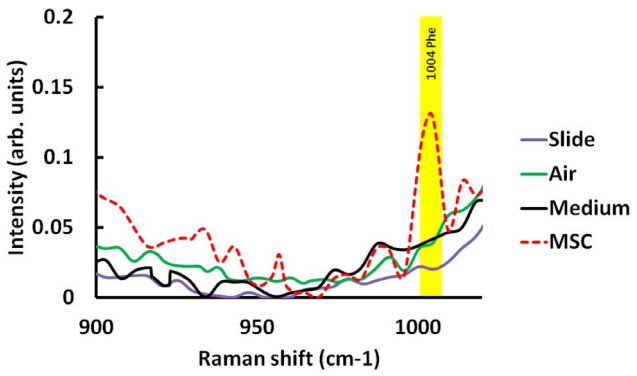

Figure 2. (A) Background signal of Raman spectra. Magnified details of the region for control and cell species from 900 to 1020 cm^{-1} in stack diagram.
doi:10.1371/journal.pone.0065438.g002

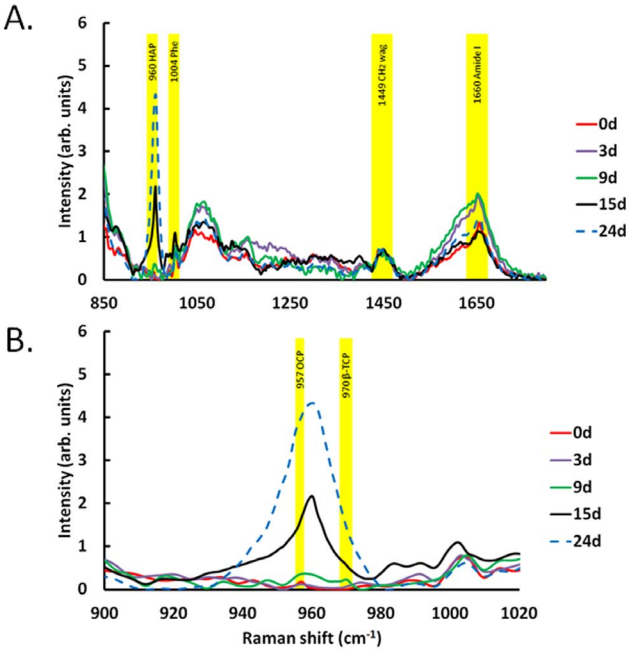

Figure 3. (A) Raman spectra of MSCs during osteogenic differentiation from 900 to 1800 cm^{-1}. (B) Magnified detail region for species from 900 to 1020 cm^{-1} in stack diagram. OCP at 957 cm^{-1} decreased upon osteogenic differentiation; β-TCP at 970 cm^{-1} transiently appeared at Day 9 and HAP at 960 cm^{-1} significantly increased after day9.
doi:10.1371/journal.pone.0065438.g003

measure the maturation level of MSC-osteoblast differentiation by detecting the intensity changes of mineral components in MSCs. However, the ACP at 952 cm^{-1} and DCPD at 985 cm^{-1} cannot be found in Figure 3A.

To further confirm the negative results of ACP and DCPD in Figure 3A, we enhanced Raman signals by increasing the integrated duration to two times and reduced the recorded range of Raman shift. The similar results were presented in Fig. 4A, OCP and β-TCP signals transiently appear, and HAP signal increases from Day 9 during MSC-osteoblast differentiation. In addition, ACP and DCPD still cannot be detected in this experiment.

Quantitative data analysis

It has been reported that mineral-to-matrix ratios (HAP/CH_2 wag) as a quantitative method to quantify the Raman signals of mineralized matrices. [62,63] In order to quantitative analyze the experimental results, we calculated the mineral-to-matrix ratios which resulting from dividing the intensity of HAP and CH_2 wag at 960 cm^{-1} (Figure 4B) and 1449 cm^{-1} (Figure 4C). As expected, Figure 4D suggests that mineral-to-matrix ratios (HAP/CH_2 wag) increases linearly and highly correlated with the osteogneic induction time and differentiation maturation level during osteogenesis in MSCs.

In Vitro analysis of MSCs under osteogenic induction

To validate the efficiency of osteogenic induction in MSCs, conventional molecular biological techniques were used to evaluate the mineralization level at different time points. Significant changes of cell morphology during MSC-osteoblast differentiation were observed on day 0, 3, 9, 15 and day 24. MSCs underwent morphological changes from spindle-like to flattened cells during osteogenic induction as shown in figure 5A. To confirm the differentiation efficiency in MSCs for Raman measurements, we evaluated the osteogenic lineage markers RUNX2, periostin and type I collagen mRNA levels in MSCs at each time point after Raman measurements. The mRNA expression levels of osteogenic lineage markers up-regulated in MSCs during osteogenic differentiation (Fig. 5B). Mineralized matrixes alkaline phosphatase and calcium phosphatase has been recognized as an early stage and mature bone cell marker that increased with the extent of osteogenic differentiation. The alkaline phosphatase staining and Von Kossa staining were used to evaluate the mineralized matrixes level in MSCs during MSC osteogenesis (Fig. 5C). These data indicated the successful induction of MSCs to differentiate into osteoblasts by our published protocol.[3,7]And the osteogenic lineage markers RUNX2, periostin and type I collagen mRNA levels of Von Kossa staining samples were detected (Fig. 5D). The qPCR data of Raman (Fig. 5B) and staining samples (Fig. 5B) show the similar expression profiles. These results indicate that Raman measurement is highly comparable with conventional methods.

Discussion

The conventional biochemical methods such as immunostaining and qPCR are widely used to evaluate the maturation level of MSC-osteoblast differentiation. However, most of biochemical methods are time-consuming, require a large amount of cells and cell fixation or lysed are needed. And the significance of histological staging is limited by inter-observer variability, in addition to the fact that the majority of mature bone cells fall into the intermediate range which is not easy to assess quantitatively. In this study, we propose and demonstrate that Raman spectroscopy can be a viable real-time, quantitative, in situ single cell biodetector for tissue engineering applications. Our results indicated that the Raman spectroscopy technique has higher sensitivity, is easier to quantitatively measure the mineralization level of cells and is more efficient than the conventional methods. Most importantly, detection via Raman spectroscopy can potentially achieved even with a single cell.

Cell morphology, gene expression of bone-related markers and staining assays of mineralization were examined to confirm the maturation of MSCs-derived osteoblasts, and we also compared those results by Raman spectroscopy. Figure 5 suggested the

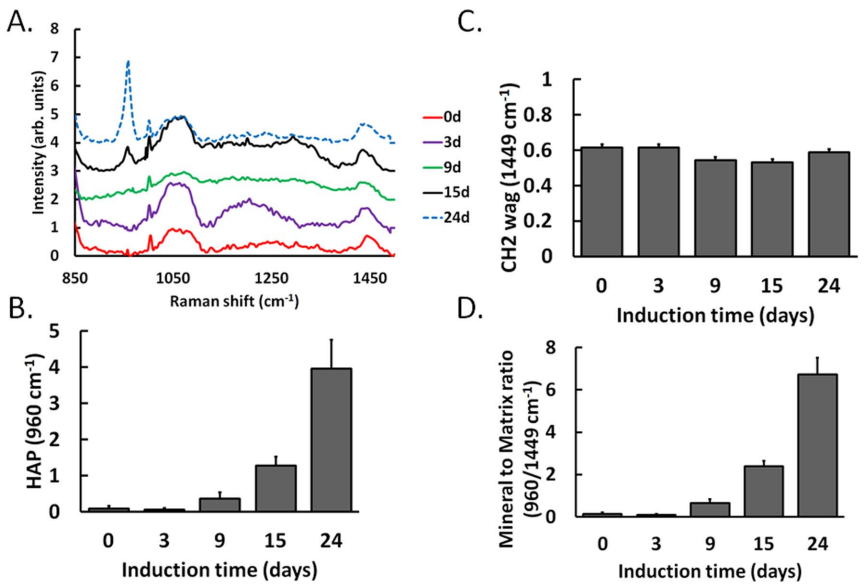

Figure 4. (A)The enhanced Raman spectra of MSCs during osteogenic differentiation from 900 to 1500 cm^{-1}. The mineral-to-matrix ratios, HAP/CH_2 wag (960/1449 cm^{-1}), divide the Raman intensity of HAP at 960 cm^{-1}(B) and CH_2 wag 1449 cm^{-1}(C). (D) The ratio significantly increased at the later stage of osteogenic induction. Data are shown as mean ± SE (n = 5).
doi:10.1371/journal.pone.0065438.g004

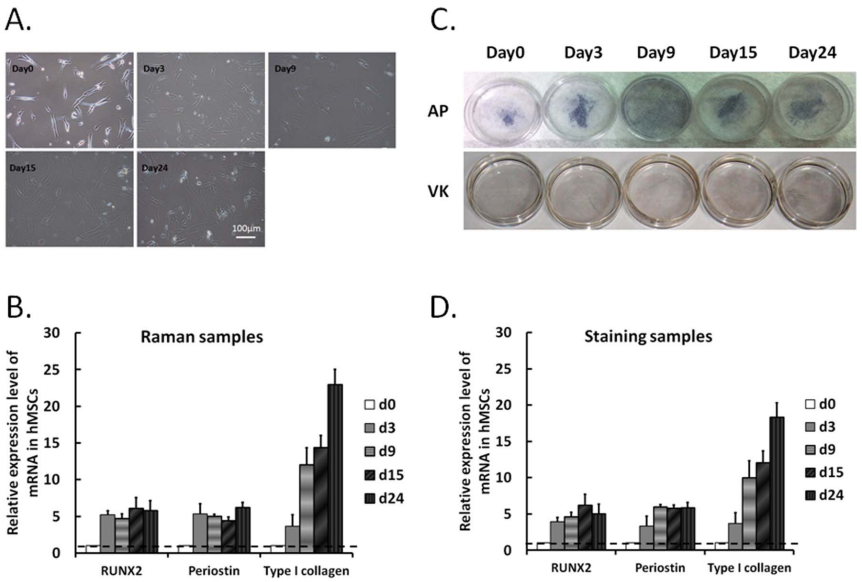

Figure 5. (A) Micrographs of MSCs treated with osteogenic media for 0, 3, 9, 15 and 24 days. (Scale bar: 100 μm) (B) Gene expression profiles of RUNX2, periostin, and type I collagen were detected in MSCs after Raman measurements by qPCR and normalized by internal and undifferentiated controls. Data are shown as mean ± SE (n = 3). (C) Alkaline phosphatase and Von Kossa staining of MSC-osteoblast differentiation. (D) Gene expression profiles of RUNX2, periostin, and type I collagen in staining samples were detected by qPCR and normalized by internal and undifferentiated controls. Data are shown as mean ± SE (n = 3).
doi:10.1371/journal.pone.0065438.g005

progression of MSCs into a more differentiated stage as mature osteoblasts as a successful osteogenic induction from MSCs.

Many of external environmental factors affect Raman signals such as the gamma rays, the dark current resulting from the thermal noise of CCD, fluorescent substances and unsuitable substrates. To evaluate and improve the stability of our Raman platform, we tested the Raman spectra of coverglass and quartz (Figure S1). Raman spectrum of coverglass has much more background noises with broad band peaks compared with the result of quartz which affects the measurement of Raman signal in MSCs. Therefore, we used quartz substrate due to its simple crystal property which provides a higher resolution of Raman measurement for cellular samples.

Raman signals of subtracts such as CH_2 wag [64], Amide I [65] and Phe [66] have been used to normalize the intensity of Raman spectrum. Phe was considered for normalization, but the signal is not consistent during MSC-osteoblast differentiation due to the contribution of Phe in non-collagenous matrix protein. The signal of Amide I at 1500 to 1800 cm^{-1} shows a broadband in Raman spectrum which also affects the data normalization. All spectra were normalized by CH_2 wag signal at 1449 cm^{-1} due to the high stability in MSCs during osteogenic induction. The Raman signals of Phe, CH_2 wag and amide I were marked in yellow (Fig. 3A).

To confirm the signal intensity of mineral species, we increased integration time to enhance Raman signals. In addition, increasing the period of experimental operation cause cell death, the recorded Raman shift was cut down to 800–1500 cm^{-1}. The enhanced signals of Raman spectra (Fig. 4A) are further improved by increasing the interrogation time compared with the results show in figure 3A.

Our results also indicate that OCP expresses in non-differentiated MSCs and significantly decreases after oeteogenic induction in MSCs. These suggest that OCP plays an essential role at early stage of mineralization during MSC-osteoblast differentiation. As the result of that, mineral-to-matrix ratio is very low in undifferentiated MSCs at day0 and day3 and significantly increases after day9.

On the other hand, β-TCP and collagen composite involved in the process of HAP synthesis as an enhancer which can be absorbed and further promote new bone formation and regeneration both *in vitro* and *in vivo*.[53,67] Our results of demonstrated that β-TCP signal transient increase at Day 9 which may highly related to the expression of type I collagen (Fig. 5B and D).

However, the signals of HAP precursors, ACP and DCPD, did not show in our Raman spectra (Fig. 3A and 4A). We suggest that might because the productions of ACP and DCPD are too low in cells to detect during osteogenic differentiation in MSCs.

In this study, we developed a method using Raman spectroscopy to evaluate the maturation level of MSCs osteoblasts differentiation by monitoring level of mineral matrix. Raman spectra including HAP at 960 cm^{-1}, OCP at 957 cm^{-1}, and β-TCP at 970 cm^{-1} were slightly different at different stages of osteogenic differentiation.

In summary, we demonstrated that Raman spectroscopy is an excellent biosensor to detect the extent of maturation during MSCs-osteoblast differentiation in a non-disruptive, real-time and label free manner. Raman spectroscopy also provides objective data at the molecular level for not only stem cell research but also for the fields of biomedicine, especially tissue regenerative medicine in the near future.

Conclusion

Although this technical platform cannot provide enough subcellular information in MSCs during oasteogenesis, base on our achievements we can introduce more powerful optical techniques such as surface-enhanced Raman scattering (SERS) and coherent anti-Stokes Raman scattering (CARS) into fields of biomedical research to further complement the deficits in traditional biological research. In this study, we established a unique detection method by using Raman spectroscopy to

evaluate osteogenic differentiation of MSCs. The Raman-based platform enables rapid, real-time and sequential evaluation in a non cell-disruptive and label free manner. This platform technology provides accurate evaluation of osteogenic maturation in a small amount of sample; it can also make possible the further investigation the mechanism of mineral deposition during bone formation. Altogether, Raman spectroscopy may facilitate future advances in bone cell biology.

Supporting Information

Figure S1 Raman spectra of coverglass and quartz for substrate. (TIF)

Author Contributions

Conceived and designed the experiments: PSH YCK. Performed the experiments: PSH YCK. Analyzed the data: PSH. Contributed reagents/materials/analysis tools: HHKC OKSL. Wrote the paper: PSH YCK HGC HHKC OKSL.

References

1. Fulmer MT, Brown PW (1998) Hydrolysis of dicalcium phosphate dihydrate to hydroxyapatite. Journal of Materials Science-Materials in Medicine 9: 197–202.
2. Jiang YH, Jahagirdar BN, Reinhardt RL, Schwartz RE, Keene CD, et al. (2002) Pluripotency of mesenchymal stem cells derived from adult marrow. Nature 418: 41–49.
3. Pittenger MF, Mackay AM, Beck SC, Jaiswal RK, Douglas R, et al. (1999) Multilineage potential of adult human mesenchymal stem cells. Science 284: 143–147.
4. Al-Khaldi A, Eliopoulos N, Martineau D, Lejeune L, Lachapelle K, et al. (2003) Postnatal bone marrow stromal cells elicit a potent VEGF-dependent neoangiogenic response in vivo. Gene Therapy 10: 621–629.
5. Lee KD, Kuo TKC, Whang-Peng J, Chung YF, Lin CT, et al. (2004) In vitro hepatic differentiation of human mesenchymal stem cells. Hepatology 40: 1275–1284.
6. Liu G, Pareta RA, Wu R, Shi Y, Zhou X, et al. (2012) Skeletal myogenic differentiation of urine-derived stem cells and angiogenesis using microbeads loaded with growth factors. Biomaterials.
7. Lee OK, Kuo TK, Chen WM, Lee KD, Hsieh SL, et al. (2004) Isolation of multipotent mesenchymal stem cells from umbilical cord blood. Blood 103: 1669–1675.
8. Zuk PA, Zhu M, Mizuno H, Huang J, Futrell JW, et al. (2001) Multilineage cells from human adipose tissue: Implications for cell-based therapies. Tissue Engineering 7: 211–228.
9. Villaron EM, Almeida J, Lopez-Holgado N, Alcoceba M, Sanchez-Abarca LI, et al. (2004) Mesenchymal stem cells are present in peripheral blood and can engraft after allogeneic hematopoietic stem cell transplantation. Haematologica 89: 1421–1427.
10. Tondreau T, Meuleman N, Delforge A, Dejeneffe M, Leroy R, et al. (2005) Mesenchymal stem cells derived from CD133-positive cells in mobilized peripheral blood and cord blood: Proliferation, Oct4 expression, and plasticity. Stem Cells 23: 1105–1112.
11. Salem HK, Thiemermann C (2010) Mesenchymal Stromal Cells: Current Understanding and Clinical Status. Stem Cells 28: 585–596.
12. Kuo TK, Ho JH, Lee OK (2009) Mesenchymal Stem Cell Therapy for Nonmusculoskeletal Diseases: Emerging Applications. Cell Transplantation 18: 1013–1028.
13. Ohgushi H, Kotobuki N, Funaoka H, Machida H, Hirose M, et al. (2005) Tissue engineered ceramic artificial joint - ex vivo osteogenic differentiation of patient mesenchymal cells on total ankle joints for treatment of osteoarthritis. Biomaterials 26: 4654–4661.
14. Zou XH, Cai HX, Yin Z, Chen X, Jiang YZ, et al. (2009) A Novel Strategy Incorporated the Power of Mesenchymal Stem Cells to Allografts for Segmental Bone Tissue Engineering. Cell Transplantation 18: 433–441.
15. Calvi LM, Adams GB, Weibrecht KW, Weber JM, Olson DP, et al. (2003) Osteoblastic cells regulate the haematopoietic stem cell niche. Nature 425: 841–846.
16. Deng ZL, Sharff KA, Tang N, Song WX, Luo JY, et al. (2008) Regulation of osteogenic differentiation during skeletal development. Frontiers in Bioscience-Landmark 13: 2001–2021.
17. Nishimura R, Hata K, Ikeda F, Ichida F, Shimoyama A, et al. (2008) Signal transduction and transcriptional regulation during mesenchymal cell differentiation. Journal of Bone and Mineral Metabolism 26: 203–212.
18. Maul TM, Chew DW, Nieponice A, Vorp DA (2011) Mechanical stimuli differentially control stem cell behavior: morphology, proliferation, and differentiation. Biomechanics and Modeling in Mechanobiology 10: 939–953.
19. Kuo SW, Lin HI, Ho JH, Shih YR, Chen HF, et al. (2012) Regulation of the fate of human mesenchymal stem cells by mechanical and stereo-topographical cues provided by silicon nanowires. Biomaterials 33: 5013–5022.
20. Mcculloch CAG, Tenenbaum HC (1986) Dexamethasone Induces Proliferation and Terminal Differentiation of Osteogenic Cells in Tissue-Culture. Anatomical Record 215: 397–402.
21. Rodriguez JP, Gonzalez M, Rios S, Cambiazo V (2004) Cytoskeletal organization of human mesenchymal stem cells (MSC) changes during their osteogenic differentiation. Journal of Cellular Biochemistry 93: 721–731.
22. Boskey AL (1992) Mineral-Matrix Interactions in Bone and Cartilage. Clinical Orthopaedics and Related Research: 244–274.
23. Johnsson MSA, Nancollas GH (1992) The Role of Brushite and Octacalcium Phosphate in Apatite Formation. Critical Reviews in Oral Biology & Medicine 3: 61–82.
24. Sauer GR, Zunic WB, Durig JR, Wuthier RE (1994) Fourier-Transform Raman-Spectroscopy of Synthetic and Biological Calcium Phosphates. Calcified Tissue International 54: 414–420.
25. Penel G, Leroy N, Van Landuyt P, Flautre B, Hardouin P, et al. (1999) Raman microspectrometry studies of brushite cement: In vivo evolution in a sheep model. Bone 25: 81s–84s.
26. Fu S, Ni P, Wang B, Chu B, Peng J, et al. (2012) In vivo biocompatibility and osteogenesis of electrospun poly(epsilon-caprolactone)-poly(ethylene glycol)-poly(epsilon-caprolactone)/nano-hydroxyapatite composite scaffold. Biomaterials 33: 8363–8371.
27. Panetta NJ, Gupta DM, Quarto N, Longaker MT (2009) Mesenchymal cells for skeletal tissue engineering. Panminerva Medica 51: 25–41.
28. Cheng MT, Yang HW, Chen TH, Lee OKS (2009) Modulation of Proliferation and Differentiation of Human Anterior Cruciate Ligament-Derived Stem Cells by Different Growth Factors. Tissue Engineering Part A 15: 3979–3989.
29. Shih YRV, Chen CN, Tsai SW, Wang YJ, Lee OK (2006) Growth of mesenchymal stem cells on electrospun type I collagen nanofibers. Stem Cells 24: 2391–2397.
30. Li QB, Xu Z, Zhang NW, Zhang L, Wang F, et al. (2005) In vivo and in situ detection of colorectal cancer using Fourier transform infrared spectroscopy. World J Gastroenterol 11: 327–330.
31. Huang Z, McWilliams A, Lui H, McLean DI, Lam S, et al. (2003) Near-infrared Raman spectroscopy for optical diagnosis of lung cancer. Int J Cancer 107: 1047–1052.
32. Chan JW, Taylor DS, Lane SM, Zwerdling T, Tuscano J, et al. (2008) Nondestructive identification of individual leukemia cells by laser trapping Raman spectroscopy. Anal Chem 80: 2180–2187.
33. Chan JW, Taylor DS, Zwerdling T, Lane SM, Ihara K, et al. (2006) Micro-Raman spectroscopy detects individual neoplastic and normal hematopoietic cells. Biophys J 90: 648–656.
34. Hughes C, Liew M, Sachdeva A, Bassan P, Dumas P, et al. (2010) SR-FTIR spectroscopy of renal epithelial carcinoma side population cells displaying stem cell-like characteristics. Analyst 135: 3133–3141.
35. Walsh MJ, Fellous TG, Hammiche A, Lin WR, Fullwood NJ, et al. (2008) Fourier transform infrared microspectroscopy identifies symmetric PO(2)(-) modifications as a marker of the putative stem cell region of human intestinal crypts. Stem Cells 26: 108–118.
36. Zhao R, Quaroni L, Casson AG (2010) Fourier transform infrared (FTIR) spectromicroscopic characterization of stem-like cell populations in human esophageal normal and adenocarcinoma cell lines. Analyst 135: 53–61.
37. Gough JE, Notingher I, Hench LL (2004) Osteoblast attachment and mineralized nodule formation on rough and smooth 45S5 bioactive glass monoliths. Journal of Biomedical Materials Research Part A 68A: 640–650.
38. Notingher I, Jell G, Lohbauer U, Salih V, Hench LL (2004) In situ non-invasive spectral discrimination between bone cell phenotypes used in tissue engineering. Journal of Cellular Biochemistry 92: 1180–1192.
39. Schulze HG, Konorov SO, Caron NJ, Piret JM, Blades MW, et al. (2010) Assessing Differentiation Status of Human Embryonic Stem Cells Noninvasively Using Raman Microspectroscopy. Analytical Chemistry 82: 5020–5027.
40. Notingher I, Bisson I, Bishop AE, Randle WL, Polak JMP, et al. (2004) In situ spectral monitoring of mRNA translation in embryonic stem cells during differentiation in vitro. Analytical Chemistry 76: 3185–3193.
41. Chiang HK, Peng FY, Hung SC, Feng YC (2009) In situ Raman spectroscopic monitoring of hydroxyapatite as human mesenchymal stem cells differentiate into osteoblasts. Journal of Raman Spectroscopy 40: 546–549.
42. Neugebauer U, Bocklitz T, Clement JH, Krafft C, Popp J (2010) Towards detection and identification of circulating tumour cells using Raman spectroscopy. Analyst 135: 3178–3182.
43. Eppert K, Wunder JS, Aneliunas V, Kandel R, Andrulis IL (2005) Von Willebrand factor expression in osteosarcoma metastasis. Modern Pathology 18: 388–397.
44. Murase M, Kano M, Tsukahara T, Takahashi A, Torigoe T, et al. (2009) Side population cells have the characteristics of cancer stem-like cells/cancer-initiating cells in bone sarcomas. British Journal of Cancer 101: 1425–1432.

45. Hantusch B, Kalt R, Krieger S, Puri C, Kerjaschki D (2007) Sp1/Sp3 and DNA-methylation contribute to basal transcriptional activation of human podoplanin in MG63 versus Saos-2 osteoblastic cells. Bmc Molecular Biology 8.
46. Jain R, Agarwal A, Kierski PR, Schurr MJ, Murphy CJ, et al. (2013) The use of native chemical functional groups presented by wound beds for the covalent attachment of polymeric microcarriers of bioactive factors. Biomaterials 34: 340–352.
47. Mok PL, Cheong SK, Leong CF (2008) In-vitro differentiation study on isolated human mesenchymal stem cells. Malays J Pathol 30: 11–19.
48. Kawai T, Anada T, Honda Y, Kamakura S, Matsui K, et al. (2009) Synthetic octacalcium phosphate augments bone regeneration correlated with its content in collagen scaffold. Tissue Eng Part A 15: 23–32.
49. Hennessy KM, Pollot BE, Clem WC, Phipps MC, Sawyer AA, et al. (2009) The effect of collagen I mimetic peptides on mesenchymal stem cell adhesion and differentiation, and on bone formation at hydroxyapatite surfaces. Biomaterials 30: 1898–1909.
50. Sawyer AA, Weeks DM, Kelpke SS, McCracken MS, Bellis SL (2005) The effect of the addition of a polyglutamate motif to RGD on peptide tethering to hydroxyapatite and the promotion of mesenchymal stem cell adhesion. Biomaterials 26: 7046–7056.
51. Alge DL, Santa Cruz G, Goebel WS, Chu TM (2009) Characterization of dicalcium phosphate dihydrate cements prepared using a novel hydroxyapatite-based formulation. Biomed Mater 4: 025016.
52. Tarnowski CP, Ignelzi MA, Jr., Morris MD (2002) Mineralization of developing mouse calvaria as revealed by Raman microspectroscopy. J Bone Miner Res 17: 1118–1126.
53. Stewart S, Shea DA, Tarnowski CP, Morris MD, Wang D, et al. (2002) Trends in early mineralization of murine calvarial osteoblastic cultures: a Raman microscopic study. Journal of Raman Spectroscopy 33: 536–543.
54. McManus LL, Burke GA, McCafferty MM, O'Hare P, Modreanu M, et al. (2011) Raman spectroscopic monitoring of the osteogenic differentiation of human mesenchymal stem cells. Analyst 136: 2471–2481.
55. Morris MD, Mandair GS (2011) Raman Assessment of Bone Quality. Clinical Orthopaedics and Related Research 469: 2160–2169.
56. Gentleman E, Swain RJ, Evans ND, Boonrungsiman S, Jell G, et al. (2009) Comparative materials differences revealed in engineered bone as a function of cell-specific differentiation. Nature Materials 8: 763–770.
57. Carey DM, Korenowski GM (1998) Measurement of the Raman spectrum of liquid water. Journal of Chemical Physics 108: 2669–2675.
58. Aubin JE (2001) Regulation of osteoblast formation and function. Rev Endocr Metab Disord 2: 81–94.
59. Alt KW (2002) Principles of bone biology, 2nd edition. Homo-Journal of Comparative Human Biology 53: 191–192.
60. Anada T, Kumagai T, Honda Y, Masuda T, Kamijo R, et al. (2008) Dose-dependent osteogenic effect of octacalcium phosphate on mouse bone marrow stromal cells. Tissue Eng Part A 14: 965–978.
61. Vani R, Girija EK, Elayaraja K, Prakash Parthiban S, Kesavamoorthy R, et al. (2009) Hydrothermal synthesis of porous triphasic hydroxyapatite/(alpha and beta) tricalcium phosphate. J Mater Sci Mater Med 20 Suppl 1: S43–48.
62. McManus LL, Bonnier F, Burke GA, Meenan BJ, Boyd AR, et al. (2012) Assessment of an osteoblast-like cell line as a model for human primary osteoblasts using Raman spectroscopy. Analyst 137: 1559–1569.
63. Masse PG, Boskey AL, Ziv I, Hauschka P, Donovan SM, et al. (2003) Chemical and biomechanical characterization of hyperhomocysteinemic bone disease in an animal model. BMC Musculoskelet Disord 4: 2.
64. Ager JW, Nalla RK, Breeden KL, Ritchie RO (2005) Deep-ultraviolet Raman spectroscopy study of the effect of aging on human cortical bone. J Biomed Opt 10: 034012.
65. Nemecek D, Stepanek J, Thomas GJ, Jr. (2013) Raman spectroscopy of proteins and nucleoproteins. Curr Protoc Protein Sci Chapter 17: Unit17 18.
66. Yu YP, Lei P, Hu J, Wu WH, Zhao YF, et al. (2010) Copper-induced cytotoxicity: reactive oxygen species or islet amyloid polypeptide oligomer formation. Chem Commun (Camb) 46: 6909–6911.
67. Brkovic BMB, Prasad HS, Rohrer MD, Konandreas G, Agrogiannis G, et al. (2012) Beta-tricalcium phosphate/type I collagen cones with or without a barrier membrane in human extraction socket healing: clinical, histologic, histomorphometric, and immunohistochemical evaluation. Clinical Oral Investigations 16: 581–590.